Enantiospecificity of Glutamate Carboxypeptidase II Inhibition

Takashi Tsukamoto,* Pavel Majer, Dilrukshi Vitharana, Chiyou Ni, Bunda Hin, Xi-Chun M. Lu, Ajit G. Thomas, Krystyna M. Wozniak, David C. Calvin, Ying Wu, Barbara S. Slusher, David Scarpetti, and George W. Bonneville

Guilford Pharmaceuticals Inc., 6611 Tributary Street, Baltimore, Maryland 21224

Received September 13, 2004

Two representative glutamate carboxypeptidase II (GCP II) inhibitors, 2-(hydroxypentafluorophenylmethyl-phosphinoylmethyl)pentanedioic acid **2** and 2-(3-mercaptopropyl)pentanedioic acid **3**, were synthesized in high optical purities (>97%ee). The two enantiomers of **2** were prepared from previously reported chiral intermediates, (*R*)- and (*S*)-2-(hydroxyphosphinoylmethyl)pentanedioic acid benzyl esters **8**. The synthesis of (*R*)- and (*S*)-**3** involves the hydrolysis of (*R*)- and (*S*)-3-(2-oxo-tetrahydro-thiopyran-3-yl)propionic acids, (*R*)- and (*S*)-**11**, the corresponding optically pure thiolactones delivered by chiral chromatographic separation of the racemic **11**. GCP II inhibitory assay revealed that (*S*)-**2** is 40-fold more potent than (*R*)-**2**. In contrast, both enantiomers of **3** inhibited GCP II with nearly equal potency. The efficacy observed in subsequent animal studies with these enantiomers correlated well with the inhibitory potency in a GCP II assay.

Introduction

In the brain, glutamate carboxypeptidase II (GCP II, EC 3.4.17.21) hydrolyzes *N*-acetylaspartylglutamate (NAAG) into *N*-acetylaspartate and glutamate.[1] Because of this function, the enzyme has previously been referred to as *N*-acetylated alpha-linked acidic dipeptidase (NAALADase). As NAAG is believed to be one of the major sources of glutamate in the nervous system, there has been a substantial interest in the discovery of potent and selective GCP II inhibitors for the treatment of neurological disorders associated with glutamate excitotoxicity such as stroke, spinal cord injury, amyotrophic lateral sclerosis (ALS), peripheral neuropathies, chronic pain, schizophrenia, and epilepsy.[2]

A prototype GCP II inhibitor, 2-(phosphonomethyl)-pentanedioic acid (2-PMPA **1**; Chart 1),[3] has been extensively utilized in models studying the mechanism and physiological role of GCP II as well as the potential therapeutic effects of GCP II inhibition.[4,5] While these studies have demonstrated the potential therapeutic benefit of GCP II inhibition, its poor pharmacokinetic profile has prompted us and other groups to explore other small molecule GCP II inhibitors. Using **1** as a template, we have extended our SAR (structure−activity relationship) studies to other zinc binding groups and have identified two structurally distinct GCP II inhibitors, 2-(hydroxy-pentafluorophenylmethyl-phosphinoylmethyl)pentanedioic acid **2**[6] and 2-(3-mercaptopropyl)-pentanedioic acid **3**.[7] The phosphinate-based inhibitor **2**, which inhibits the metallopeptidase GCP II by coordinating with the active site zinc atom(s), is highly water-soluble and stable in media commonly used for intravenous administration. Indeed, compound **2** shows neuroprotective effects in the rat middle cerebral artery occlusion (MCAO) model by intravenous administration.[6,8] 2-(3-Mercaptopropyl)pentanedioic acid **3** represents another class of inhibitors and exhibits the inhibitory effects through the interaction of its sulfhydryl group with the active site zinc atom(s). More importantly, compound **3** is the first reported orally bioavailable GCP II inhibitor and exhibits antinociceptive effects in a rat chronic constrictive injury (CCI) model of neuropathic pain by daily oral administration,[7] thereby potentially extending the therapeutic utility of GCP II inhibitors to multiple chronic disorders associated with glutamate excitotoxicity. Consequently, we found that the treatment of G93A FALS (familial amyotrophic lateral sclerosis) transgenic mice with **3** by oral administration results in statistically significant prolongation in median survival.[9]

Chart 1. Representative GCP II Inhibitors

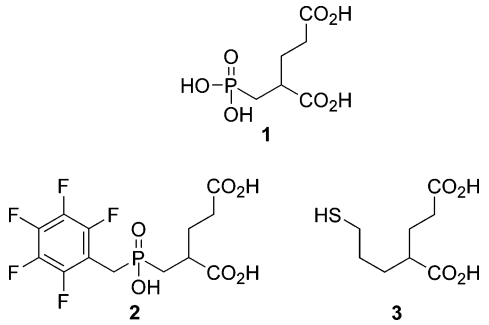

Both of these representative GCP II inhibitors were previously provided as racemates for the pharmacological evaluation. Recently, studies on the two enantiomers of 2-PMPA **1** have revealed that potent inhibition of GCP II is specific to (*S*)-2-PMPA, which has an absolute configuration corresponding to L-glutamate.[10] The results suggest that only single enantiomers of **2** and **3** potently inhibit GCP II, and therefore it is essential to identify the active enantiomers of **2** and **3** prior to further preclinical characterization in order to eliminate the potential for undesired pharmacological effects by the inactive enantiomer. In this paper, we report the

* To whom correspondence should be addressed. Phone: (410) 631−6762. Fax: (410) 631−6797. E-mail: tsukamotot@guilfordpharm.com.

10.1021/jm049258g CCC: $30.25
Published on Web 02/19/2005

Scheme 1. Synthesis of (±)-**2**[a]

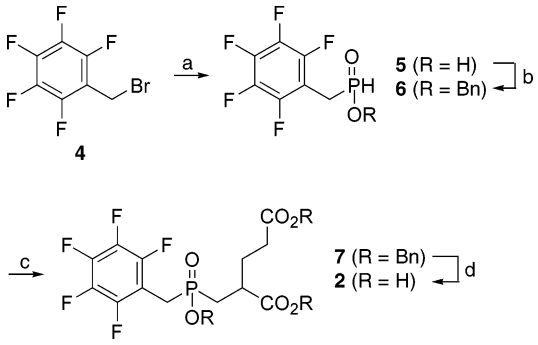

[a] Reagents and conditions: (a) BTSP, CH_2Cl_2. rt, 21%; (b) BnOH, EDC, CH_2Cl_2, rt, 28%; (c) dibenzyl 2-methyleneglutarate, NaH, THF, rt, 39%; (d) H_2, Pd/C, H_2O−THF, rt, 85%.

Scheme 2. Synthesis of (*R*)- and (*S*)-**2**[a]

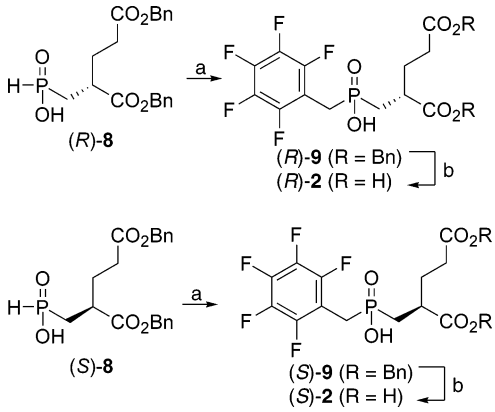

[a] Reagents and conditions: (a) **4**, TMSCl, triethylamine, CH_2Cl_2, 35 °C, >100% crude yield for (*R*)-**9**, 97% crude yield for (*S*)-**9**, (b) aq NaOH, rt, 42% for (*R*)-**2**, 61% for (*S*)-**2**.

synthesis of both enantiomers of the phosphinate-based compound **2** and the thiol-based compound **3**. Biological evaluation of these compounds in a GCP II assay and animal models of neurological disorders will be also described.

Chemistry

The original synthesis of racemic **2** is outlined in Scheme 1.[6] Pentafluorobenzyl bromide **4** was treated with bis(trimethylsilyl)phosphonite (BTSP) generated in situ to afford phosphinic acid **5**. This material was converted into benzyl ester **6**. Michael addition of **6** to dibenzyl 2-methyleneglutarate gave the tribenzyl ester derivative **7**, which was converted into **2** by catalytic hydrogenation. The penultimate step (synthesis of **7**) of this synthetic route not only creates a chiral center of our interest (α-carbon of glutarate moiety) but also turns the phosphorus atom into the second chiral center, thus providing **7** as a mixture of four diastereomers. This stereochemical complexity makes this synthetic route unfeasible for the synthesis of the enantiomers of **2** and prompted us to explore alternative synthetic routes.

We have previously reported the preparation of both enantiomers of hydroxyphosphinylmethyl-pentanedioic dibenzyl ester **8** with defined absolute configurations (Scheme 2).[10] These compounds were successfully utilized for the synthesis of (*R*)- and (*S*)-**1** and also should serve as ideal chiral intermediates for the synthesis of **2** provided that a pentafluorophenylmethyl group can

Scheme 3. Synthesis of (*R*)- and (*S*)-**11**[a]

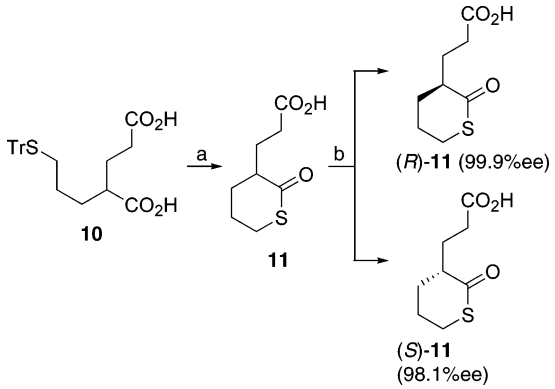

[a] Reagents and conditions: (a) (i) triethylsilane, TFA, CH_2Cl_2, 45 °C; (ii) 10-camphorsulfonic acid, toluene, reflux, 38% for two steps; (b) chiral separation, 43% for (*R*)-**11**, 42% for (*S*)-**11**.

be easily attached to the phosphorus atom of **8**. As illustrated in Scheme 2, this coupling reaction was successfully accomplished by using a procedure similar to the one reported by Reiter's group.[11] Thus, treatment of (*R*)-**8** with chlorotrimethylsilane and triethylamine in the presence of benzyl bromide **4** afforded (*R*)-**9** in quantitative crude yield. Complete elimination of oxygen from the reaction media is essential for preventing the phosphonate byproduct formation. A subsequent base-mediated hydrolysis of (*R*)-**9** gave (*R*)-**2** in 42% yield. The other enantiomer (*S*)-**2** was successfully obtained in a similar manner using (*S*)-**8** as a starting material in 61% yield. Both final products (*R*)- and (*S*)-**2** were shown to be of high optical purity (>98%ee) by chiral HPLC analysis. In addition to its capacity to produce enantiomers, the new synthetic route offers several advantages over the conventional route such as reduced number of steps and higher overall yield. The shortened route is particularly attractive as it allows us to synthesize a wide variety of optically pure phosphinate-based GCP II inhibitors in two steps by substituting other electrophilic reagents for pentafluorobenzyl bromide **4**.

Our initial attempt to prepare two enantiomers of **3** involved direct separation of racemate **3** by chiral chromatography. After unsatisfactory attempts to separate the two enantiomers in practical quantities, however, we shifted our focus to the corresponding thiolactone **11** expecting that its cyclic system would increase the degree of enantioseparation by chiral chromatography. The thiolactone **11** was readily prepared from *S*-trityl derivative **10** (Scheme 3). Chiral separation of the racemic thiolactone **11** was successfully achieved on a CHIRALPAK AD column using supercritical fluid chromatography with carbon dioxide/methanol (85/15, v/v) as a mobile phase to give (*R*)-**11** in 99.9%ee and (S)-**11** in 98.1%ee, respectively. The stereochemistry at C-2 of thiolactone **11** was established by X-ray structure analysis of (*R*)-**11** as shown in Figure 1.

Acid-mediated hydrolysis of thiolactone (*R*)-**11** to (*R*)-**3** (step a in Scheme 4) resulted in formation of completely racemized final product **3**. Under the basic conditions (step b in Scheme 4), compound (*R*)-**3** was consistently obtained in slightly lower optical purity (~90%ee) compared to that of the starting material (*R*)-**11**. Since we observed that the level of racemization is independent of reaction time, we believe that racemization

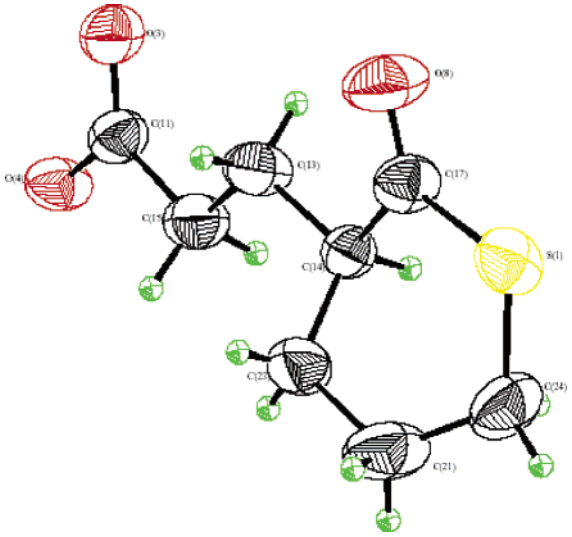

Figure 1. Crystal structure of (*R*)-(−)-**11**.

Scheme 4. Synthesis of (*R*)-**3** and (*S*)-**3**[a]

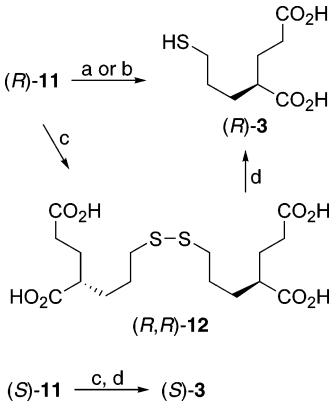

[a] Reagents and conditions: (a) 6 M HCl, 100 °C, 0%ee; (b) NaOH, dioxane−H_2O, rt, ∼90%ee; (c) LiOH, H_2O_2, rt; (d) TCEP, H_2O, rt, 97.1%ee for (*R*)-**3**, 97.5%ee for (*S*)-**3**.

occurs prior to cleavage of thiolactone **11**, which possesses a relatively acidic α-proton compared to **3**. To prevent the partial racemization, we applied Evans's procedure[12] to hydrolyze thioesters. Treatment of (*R*)-**11** with lithium hydroxide and hydrogen peroxide gave the disulfide derivative (*R*,*R*)-**12**. The formation of disulfide bond can be attributed to hydrogen peroxide-mediated oxidation of free thiol. The disulfide (*R*,*R*)-**12** was converted into (*R*)-**3** using tris(carboxyethyl)phosphine (TCEP). Chiral HPLC analysis of the product revealed that the two-step procedure provides the product with minimal racemization, yielding (*R*)-**3** in 97.1%ee. In a similar manner using (*S*)-**11** as a starting material, the other enantiomer (*S*)-**3** was obtained in 97.5%ee.

Biological Results and Discussion

In Vitro GCP II Assay. Inhibitory potencies of these enantiomers were evaluated using *N*-acetyl-L-aspartyl-[^{3}H]-L-glutamate as a substrate[13] and a purified recombinant GCP II.[14] The results are summarized in Table 1 along with previously reported values[10] for (*RS*)-, (*R*)-, and (*S*)-**1** for comparison purposes.

In a GCP II assay, (*R*)-**2** was a relatively weak inhibitor with an IC_{50} value of 1400 nM while (*S*)-**2** displayed nearly 40-fold greater inhibitory potency with an IC_{50} value of 34 nM. Significant difference in IC_{50} values between the two compounds demonstrates that the potent inhibition of GCP II by **2** is attributable to its *S*-enantiomer, which has an absolute configuration corresponding to L-glutamate. The same trend was previously observed with the two enantiomers of 2-PMPA (*R*)-**1** and (*S*)-**1** with IC_{50} values of 30 nM and 0.1 nM, respectively.[10]

Table 1. Inhibition of GCP II and Neuroprotective Effects in a Tissue Culture Model of Ischemia

compd	IC_{50} (nM)	EC_{50} (nM)
(*RS*)-**1**[a]	0.3	1.2
(*R*)-**1**[a]	30	70
(*S*)-**1**[a]	0.1	0.2
(*RS*)-**2**[b]	82 ± 14	9.5 (11; 8.0)
(*R*)-**2**[b]	1400 (1190; 1530)	410 (584, 227)
(*S*)-**2**[b]	34 ± 18	4.1 ± 1.5
(*RS*)-**3**[b]	90 ± 26	13 ± 6
(*R*)-**3**[b]	85 ± 33	nd[c]
(*S*)-**3**[b]	67 ± 29	nd[c]

[a] Values have been previously reported (ref 10) and are included herein for reference purposes. [b] Values are the mean ± SD for experiments performed at least in triplicate. When only two separate experiments were performed, values are expressed as the mean of duplicate determinations followed by each measurement separated by a semicolon in parentheses. [c] Not determined.

Surprisingly, no significant difference in GCP II inhibitory potency was observed between (*R*)-**3** and (*S*)-**3** with IC_{50} values of 85 nM and 67 nM, respectively. The lack of enantiospecificity observed with the thiol-based inhibitor **3** is unexpected, considering the evident enantiospecificity demonstrated by the two phosphorus-based inhibitors **1** and **2**. To assess the possibility of racemization under the GCP II assay conditions, we incubated (*S*)-**3** with the assay components for 15 min. Chiral HPLC analysis of the resulting assay mixture showed no sign of racemization.

The loss of enantiospecificity cannot be solely attributed to the change of the zinc-binding group from a phosphinate to a thiol group. For example, a thiol-based drug, (2*S*)-1-(3-mercapto-2-methylpropionyl)-L-proline (captopril), is 100-fold more potent than the corresponding (2*R*) analogue in inhibiting angiotensin-converting enzyme (ACE).[15] Kozikowski's group has proposed the fixed pharmacophore model consisting of two carboxylic groups of the glutarate moiety and a zinc-binding group on the basis of their predictive GCP II structures in complex with 2-PMPA and one other phosphorus-based inhibitor.[16] Both of these compounds contain the phosphorus group linked to the chiral carbon through a single methylene unit, and the model suggests that the configuration of the chiral center has significant influence on the orientation of phosphorus group. Thus GCP II inhibition by these phosphorus-based compounds exhibits a higher enantiospecificity as demonstrated by the compounds **1** and **2**. We presume that the lack of enantiospecificity observed with **3** is at least partially associated with the flexible alkyl chain linker consisting of three methylene units between the thiol group and the chiral carbon. Regardless of its absolute configuration, the flexible linker could allow the thiol group to gain the same degree of interaction with an active site zinc atom while its glutarate group optimally interacts with glutamate recognition site of the enzyme, thus resulting in equally potent inhibition by the two enantiomers of **3**.

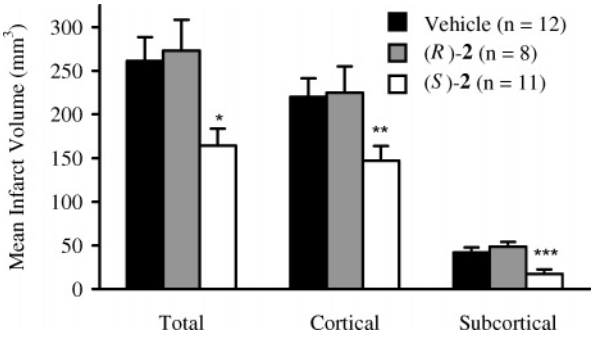

Figure 2. Reduction of ischemic injury by (*R*)- and (*S*)-**2** in the rat MCAO model. (*R*)-**2** was dosed at 30 mg/kg bolus iv (1 h postoclusion) then at 20 mg/kg/h iv for 22 h. (*S*)-**2** was dosed at 3 mg/kg bolus iv (1 h postoclusion) then at 2 mg/kg/h iv for 22 h. *37% protection ($p = 0.009$), **33% protection ($p = 0.016$), ***59% protection ($p = 0.005$).

Cell Culture Model of Cerebral Ischemia. Since compound **2** was intended for the treatment of ischemic stroke, the two enantiomers of **2** were also tested in an established tissue culture model of cerebral ischemia.[17] In this model, rat cortical cultures were exposed to potassium cyanide and 2-deoxyglucose to simulate ischemia. Cellular injury was quantified by measurement of cytosolic lactate dehydrogenase released into medium. As shown in Table 1, (*RS*)-**2** and (*S*)-**2** exhibited strong neuroprotection against ischemic injury with median effective concentration (EC_{50}) values of 9.5 nM and 4.1 nM, respectively. (*R*)-**2** exhibited much weaker potency in this model with an EC_{50} value of 410 nM. The good correlation between GCP II inhibitory and neuroprotective potencies of (*R*)-**2** (less potent in both assays) and (*S*)-**2** (more potent in both assays) provides further experimental evidence that the neuroprotective effect of these compounds is due to their ability to inhibit GCP II.

Neuroprotective Effects of (*R*)- and (*S*)-2 in the Rat Middle Cerebral Artery Occlusion (MCAO) Model. The two enantiomers (*R*)- and (*S*)-**2** were evaluated for neuroprotection against ischemic injury in a transient middle cerebral artery occlusion model in the anesthetized rat (Figure 2). The less potent enantiomer (*R*)-**2** was given in bolus (30 mg/kg iv) at 1 h after occlusion followed by continuous infusion (20 mg/kg/h iv) for 22 h. The more potent enantiomer (*S*)-**2** was given in a similar manner but at 10-fold lower dose (3 mg/kg bolus iv then 2 mg/kg/h iv). As shown in Figure 2, treatment with (*R*)-**2** produced no effect on ischemic core infarction volumes. On the other hand, significant reduction in the volume of ischemic injury was observed in both cortical and subcortical regions of animals treated with more potent enantiomer (*S*)-**2**.

Antinociceptive Effects of (*R*)- and (*S*)-3 in the Rat Chronic Constriction Injury (CCI) Model. The two enantiomers (*R*)- and (*S*)-**3** were evaluated for their antinociceptive effects using the rat chronic constriction injury (CCI) model[18] of neuropathic pain by oral administration. Since the two enantiomers are equally potent GCP II inhibitors, both of them were tested at 10 mg/kg/day by oral administration, the minimally effective dose for the racemate (±)-**3** from the previously conducted studies.[7] Figure 3 summarizes the results of the studies with (*R*)-**3** (Figure 3A) and (*S*)-**3** (Figure 3B). Although onset of antinociceptive effect was different

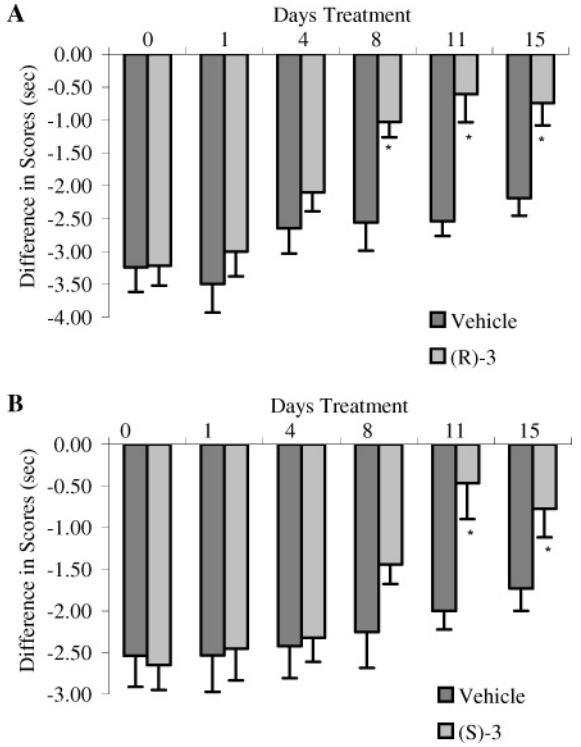

Figure 3. Antinociceptive effects of (*R*)- and (*S*)-**3** (10 mg/kg/day, po) in the rat chronic constriction injury (CCI) model of neuropathic pain. Both (*R*)-**3** (A) and (*S*)-**3** (B) significantly attenuated CCI-induced hyperalgesic state relative to the vehicle-treated control (*$p < 0.05$).

by one measurement time point, both (*R*)-**3** and (*S*)-**3** significantly attenuated CCI-induced hyperalgesic state relative to the vehicle-treated control. The fact that both (*R*)- and (*S*)-**3** as well as (±)-**3** exhibit a similar in vivo efficacy profile suggests that the two enantiomers not only inhibit GCP II with equal potency but also share a similar pharmacokinetic profile when administered orally.

Conclusions

The MCAO model of stroke in rats has demonstrated a marked difference in efficacy between the two enantiomers of **2**, with (*S*)-**2** providing superior neuroprotection. Furthermore, the similarly potent enantiomers (*R*)- and (*S*)-**3** showed comparable efficacy in the neuropathic pain model. A good correlation between GCP II potency and in vivo efficacy of these compounds supports GCP II inhibition as the underlying mechanisms of action in these animal models. As far as the phosphinate-based inhibitor **2** is concerned, our studies clearly suggest that further drug development activity should be conducted exclusively with the more potent enantiomer (*S*)-**2**. As for the thiol-based inhibitor **3**, additional comparative assessment (e.g., toxicology) of the two enantiomers will be required prior to selection of a single enantiomer for clinical development.

Experimental Section

^{1}H, ^{13}C, and ^{31}P NMR spectra were recorded on a Bruker DRX-400 instrument at 400, 100, and 162 MHz, respectively. Optical purity analyses were performed on a Jasco HPLC system equipped with a chiral chromatography column. Elemental analyses were obtained from Atlantic Microlabs,

Norcross, GA, and optical rotations were obtained from Robertson Microlit Laboratories, Inc., Madison, NJ.

(*R*)-2-(Hydroxy-pentafluorophenylmethyl-phosphinoylmethyl)pentanedioic Acid Dibenzyl Ester ((*R*)-9). A solution of (*R*)-**8** (417.4 g, 1.069 mol) and **4** (161.5 mL, 1.069 mol) in dichloromethane (3.13 L) was degassed and purged with argon three times. Trimethylchlorosilane (407 mL, 3.207 mol) and triethylamine (447 mL, 3.207 mol) were added to the solution while maintaining the temperature below 20 °C. The mixture was allowed to warm to room temperature and was heated at 35 °C for 45 h. The reaction was cooled in an ice bath and quenched with water (167 mL). Water (1.503 L) was added and stirred gently over 20 min. The organic layer was separated and concentrated in vacuo to give 644.8 g of (*R*)-**9** as a light yellow oil (>100% crude yield). The crude material was used for the next step without further purification: ^{1}H NMR (CD_3OD) δ 1.8−2.1 (m, 3H), 2.2−2.5 (m, 3H), 2.8−3.0 (m, 1H), 3.25 (d, J = 15.4 Hz, 2H), 5.0−5.2 (m, 4H), 7.2−7.4 (m, 10H); ^{13}C NMR (CD_3OD) δ 25.8 (d, J = 85.9 Hz), 29.9 (d, J = 11.5 Hz), 32.1, 32.2 (d, J = 95.1 Hz), 40.0 (d, J = 3.8 Hz), 67.3, 67.9, 129.0−130.0 (multiple aromatic peaks), 137.3, 137.6, 137.0−148.0 (multiple fluoroaromatic peaks), 174.0, 175.5 (d, J = 6.9 Hz); ^{31}P NMR (CD_3OD) δ 43.0 (m).

(*R*)-2-(Hydroxy-pentafluorophenylmethyl-phosphinoylmethyl)pentanedioic Acid ((*R*)-2). The above crude product (*R*)-**9** (640 g, 1.122 mol) was dissolved in an aqueous solution of sodium hydroxide (256 g, 6.400 mol) in water (3.2 L) and cooled with an ice bath. The mixture was allowed to warm to room temperature slowly overnight and stirred for 24 h. The reaction mixture was washed with *tert*-butyl methyl ether (1 L × 3) and the aqueous phase was acidified to pH 1 with conc HCl (340 mL). The acidified aqueous phase was extracted with *tert*-butyl methyl ether (3 L × 3) after saturating with salt. The combined extracts were concentrated in vacuo and the resulting oil was azeotroped with dichloromethane (2 L). The resulting pale yellow solid was taken up in THF (2 L) and a colorless solid was filtered off. The resulting solid was taken up in 6 M HCl (1.5 L) and extracted with *tert*-butyl methyl ether (1 L × 3). The extracts were combined with the filtrate and concentrated in vacuo. The residue was triturated with 10% *tert*-butyl methyl ether in dichloromethane (2.0 L) overnight. The resulting solid was filtered and washed with dichloromethane (200 mL × 2). The solid was triturated one more time with 10% *tert*-butyl methyl ether in dichloromethane (2.0 L) for 2 days. The resulting solid was filtered and washed with dichloromethane (1.6 L). The solid was dried in vacuo at 22 °C to give 182 g of (*R*)-**2** as a white solid (42% yield for the two steps): mp 152−154 °C; ^{1}H NMR (D_2O) δ 1.7−1.9 (m, 3H), 2.09 (ddd, J = 9.1, 13.1, 15.4 Hz, 1H), 2.31 (dt, J = 16.9, 7.3 Hz, 1H), 2.36 (dt, J = 16.9, 7.3 Hz, 1H), 2.6−2.8 (m, 1H), 3.15 (d, J = 15.2 Hz); ^{13}C NMR (D_2O) δ 22.8 (d, J = 86.6 Hz), 26.5 (d, J = 12.3 Hz), 28.8 (d, J = 92.8 Hz), 29.2, 36.8 (d, J = 3.8 Hz), 134.0−145.0 (multiple fluoroaromatic peaks), 175.6, 176.6 (d, J = 6.1 Hz); ^{31}P NMR (D_2O) δ 44.9 (m); $[\alpha]^{25}_D$ = +1.85 (*c* 1.0, H_2O); 98.3%ee (CHIRALPAK AD-H 4.6 mm × 250 mm with hexanes/*i*-PrOH/TFA, 90/10/0.1). Anal. ($C_{13}H_{12}F_5O_6P$) C, H.

(*S*)-2-(Hydroxy-pentafluorophenylmethyl-phosphinoylmethyl)pentanedioic Acid ((*S*)-2). The (*S*)-enantiomer (*S*)-**2** was synthesized as described above for (*R*)-**2** except starting with (*S*)-**8** (59% yield for the two steps): mp 155−157 °C; ^{1}H, ^{13}C, and ^{31}P NMR spectral data were identical to those of (*R*)-**2**; $[\alpha]^{25}_D$ = −1.64 (*c* 1.0, H_2O); 98.6%ee (CHIRALPAK AD-H 4.6 mm × 250 mm with hexanes/*i*-PrOH/TFA, 90/10/0.1). Anal. ($C_{13}H_{12}F_5O_6P$) C, H.

3-(2-Oxo-tetrahydro-thiopyran-3-yl)propionic Acid (11). To a solution of **10** (150 g, 334 mmol) in dichloromethane (500 mL) was dropwise added trifluoroacetic acid (110 mL) over 30 min. The resulting brown solution was stirred at room temperature for additional 30 min. A solution of triethylsilane (45 mL, 0.33 mol) in dichloromethane (50 mL) was added to the mixture and stirred at 45 °C for 1h. The volatiles were removed in vacuo and the residue was triturated with hexanes (500 mL × 2). The oily residue was dissolved in toluene (500 mL) containing 10-camphorsulfonic acid (14 g, 60 mmol) and refluxed for 6 h. The generated water was removed using a Dean−Stark trap. The solvent was then removed under reduced pressure and the residue was purified by silica gel chromatography (Hexanes/EtOAc, 4:1). Fractions containing the product were collected, concentrated, and recrystallized from EtOAc/hexanes to give 23.3 g of **11** as a white solid (38% yield): mp 85−86 °C; ^{1}H NMR (CD_3OD) δ 1.62−1.75 (m, 2H), 2.00−2.15 (m, 4H), 2.30−2.45 (m, 2H), 2.60−2.70 (m, 1H), 3.13 (dt, J = 13.1, 6.0 Hz, 1H), 3.21 (dt, J = 13.1, 6.5 Hz, 1H); ^{13}C NMR (CD_3OD) δ 23.3, 27.4, 29.3, 31.2, 32.3, 50.0, 177.0, 206.4. Anal. ($C_8H_{12}O_3S$) C, H, S.

Separation of Enantiomers of 11 by Chiral Supercritical Fluid Chromatography. Racemic **11** (2.70 g, 14.3 mmol) was passed through a CHIRALPAK AD column (21 mm id × 250 mm length) using carbon dioxide/methanol (85/15, v/v) as eluent at a flow rate of 5 mL/min at 25 °C. Fractions containing the first eluting enantiomer (detected by UV at 220 nm) was concentrated to afford 1.15 g of (*R*)-**11** as a white solid (43% yield): ^{1}H and ^{13}C NMR spectral data were identical to those of (±)-**11**; mp 78−79 °C; $[\alpha]^{25}_D$ = −28.8 (*c* 1.0, CH_3CN); 99.9%ee (CHIRALPAK AD-RH 4.6 mm × 150 mm with hexanes/EtOH/TFA, 90/10/0.1). Anal. ($C_8H_{12}O_3S$) C, H, S. Concentration of fractions containing the second eluting enantiomer gave 1.13 g of (*S*)-**11** as a white solid (42% yield): ^{1}H and ^{13}C NMR spectral data were identical to those of (±)-**11**; mp 78−79 °C; $[\alpha]^{25}_D$ = +28.8 (*c* 1.0, CH_3CN); 98.1% (CHIRALPAK AD-RH 4.6 mm × 150 mm with hexanes/EtOH/TFA, 90/10/0.1). Anal. ($C_8H_{12}O_3S$) C, H, S.

(*R*)-2-(3-Mercaptopropyl)pentanedioic Acid (*R*)-3. To a solution of (*R*)-**11** (100 mg, 0.5 mmol) in H_2O-THF (v/v = 3/5, 0.8 mL) were added $LiOH{\cdot}H_2O$ (36 mg, 1.25 mmol) and H_2O_2 (30% in H_2O, 0.3 mL, 2.6 mmol) at 0 °C. The mixture was stirred at 0 °C for 3 h and quenched by the addition of saturated aq $Na_2S_2O_3$ (2.0 mL). The mixture was acidified to pH 1 by 10% aq $KHSO_4$ and extracted with diethyl ether (10.0 mL × 3). The combined extracts were washed with brine, dried over $MgSO_4$, and concentrated to give (*R*,*R*)-**12** as a colorless oil. To a solution of (*R*,*R*)-**12** in 0.5 N $NaHCO_3$ (3.0 mL) was added tris(carboxyethyl)phosphine hydrochloride (144 mg, 0.5 mmol), and the mixture was stirred at room temperature for 2 min. The reaction mixture was acidified to pH 1 with 10% $KHSO_4$ and extracted with EtOAc (10.0 mL × 3). The combined extracts were washed with brine, dried over $MgSO_4$, and concentrated to give 70 mg of (*R*)-**3** as a colorless oil (70% overall yield): ^{1}H NMR ($CDCl_3$) δ 1.35 (t, J = 7.9 Hz, 1H), 1.55−1.80 (m, 4H), 1.80−2.05 (m, 2H), 2.44 (t, J = 7.2 Hz, 2H), 2.40−2.50 (m, 1H), 2.53 (q, J = 7.1 Hz, 2H), 10.7−11.20 (br, 2H); ^{13}C NMR ($CDCl_3$) δ 24.3, 26.6, 30.5, 31.4, 31.7, 44.1, 179.4, 181.7; $[\alpha]^{25}_D$ = +1.70 (*c* 1.0, CH_3CN); 97.1%ee (CHIRALCEL OJ-H 4.6 mm × 250 mm with hexanes/*i*-PrOH/TFA, 90/10/0.1). Anal. ($C_8H_{14}O_4S{\cdot}0.25H_2O$) C, H, S.

(*S*)-2-(3-Mercaptopropyl)pentanedioic Acid (*S*)-3. The (*S*)-enantiomer (*S*)-**3** was synthesized as described above for (*R*)-**3** except starting with (*S*)-**11** (70% overall yield): ^{1}H, ^{13}C NMR spectral data were identical to those of (*R*)-**3**; $[\alpha]^{25}_D$ = −2.26 (*c* 1.0, CH_3CN); 97.5%ee (CHIRALCEL OJ-H 4.6 mm × 250 mm with hexanes/*i*-PrOH/TFA, 90/10/0.1). Anal. ($C_8H_{14}O_4S{\cdot}0.25H_2O$) C, H, S.

Biological and Pharmacological Studies. The GCP II assay[13] and cell culture model of cerebral ischemia[4,17] were carried out as outlined previously. The rat middle cerebral artery occlusion model was performed as previously described.[8] The chronic constrictive injury models were performed following the procedure reported by Bennett's group.[18]

Acknowledgment. Synthesis of both enantiomers of **2** and chiral separation of **11** were codeveloped with Oxford Asymmetry International and Chiral Technology, respectively. X-ray structure analysis of (*R*)-(−)-**11** was performed by Rigaku MSC.

Supporting Information Available: X-ray crystallographic analysis of (*R*)-**11**. This material is available free of charge via the Internet at http://pubs.acs.org.

References

(1) Carter, R. E.; Coyle, J. T. Glutamate Carboxypeptidase II. In *Handbook of Proteolytic Enzymes*, Barrett, A. J., Rawlings, N. D., Woessner, J. F., Eds. Academic: New York, 1998; pp 1434−1437.

(2) Whelan, J. NAALADase inhibitors: A novel approach to glutamate regulation. *Drug Discovery Today* **2000**, *5*, 171−172.

(3) Jackson, P. F.; Cole, D. C.; Slusher, B. S.; Stetz, S. L.; Ross, L. E.; Donzanti, B. A.; Trainor, D. A. Design, synthesis, and biological activity of a potent inhibitor of the neuropeptidase *N*-acetylated alpha-linked acidic dipeptidase. *J. Med. Chem.* **1996**, *39*, 619−622.

(4) Slusher, B. S.; Vornov, J. J.; Thomas, A. G.; Hurn, P. D.; Harukuni, I.; Bhardwaj, A.; Traystman, R. J.; Robinson, M. B.; Britton, P.; Lu, X. C.; Tortella, F. C.; Wozniak, K. M.; Yudkoff, M.; Potter, B. M.; Jackson, P. F. Selective inhibition of NAALADase, which converts NAAG to glutamate, reduces ischemic brain injury. *Nat. Med.* **1999**, *5*, 1396−1402.

(5) Chen, S. R.; Wozniak, K. M.; Slusher, B. S.; Pan, H. L. Effect of 2-(phosphono-methyl)-pentanedioic acid on allodynia and afferent ectopic discharges in a rat model of neuropathic pain. *J. Pharmacol. Exp. Ther.* **2002**, *300*, 662−667.

(6) Jackson, P. F.; Tays, K. L.; Maclin, K. M.; Ko, Y. S.; Li, W.; Vitharana, D.; Tsukamoto, T.; Stoermer, D.; Lu, X. C.; Wozniak, K.; Slusher, B. S. Design and pharmacological activity of phosphinic acid based NAALADase inhibitors. *J. Med. Chem.* **2001**, *44*, 4170−4175.

(7) Majer, P.; Jackson, P. F.; Delahanty, G.; Grella, B. S.; Ko, Y. S.; Li, W.; Liu, Q.; Maclin, K. M.; Polakova, J.; Shaffer, K. A.; Stoermer, D.; Vitharana, D.; Wang, E. Y.; Zakrzewski, A.; Rojas, C.; Slusher, B. S.; Wozniak, K. M.; Burak, E.; Limsakun, T.; Tsukamoto, T. Synthesis and biological evaluation of thiol-based inhibitors of glutamate carboxypeptidase II: discovery of an orally active GCP II inhibitor. *J. Med. Chem.* **2003**, *46*, 1989−1996.

(8) Williams, A. J.; Lu, X. M.; Slusher, B.; Tortella, F. C. Electroencephalogram analysis and neuroprotective profile of the *N*-acetylated-alpha-linked acidic dipeptidase inhibitor, GPI5232, in normal and brain-injured rats. *J. Pharmacol. Exp. Ther.* **2001**, *299*, 48−57.

(9) Ghadge, G. D.; Slusher, B. S.; Bodner, A.; Canto, M. D.; Wozniak, K.; Thomas, A. G.; Rojas, C.; Tsukamoto, T.; Majer, P.; Miller, R. J.; Monti, A. L.; Roos, R. P. Glutamate carboxypeptidase II inhibition protects motor neurons from death in familial amyotrophic lateral sclerosis models. *Proc. Natl. Acad. Sci. U.S.A.* **2003**, *100*, 9554−9559.

(10) Vitharana, D.; France, J. E.; Scarpetti, D.; Bonneville, G. W.; Majer, P.; Tsukamoto, T. Synthesis and biological evaluation of (*R*)- and (*S*)-2-(phosphonomethyl)pentanedioic acids as inhibitors of glutamate carboxypeptidase II. *Tetrahedron: Asymm.* **2002**, *13*, 1609−1614.

(11) Reiter, L. A.; Jones, B. P. Amide-assisted hydrolysis of β-carboxamido-substituted phosphinic acid esters. *J. Org. Chem.* **1997**, *62*, 2808−2812.

(12) Evans, D. A.; Wu, L. D.; Wiener, J. J. M.; Johnson, J. S.; Ripin, D. H. B.; Tedrow, J. S. A general method for the synthesis of enantiomerically pure β-substituted, β-amino acids through α-substituted succinic acid derivatives. *J. Org. Chem.* **1999**, *64*, 6411−6417.

(13) Rojas, C.; Frazier, S. T.; Flanary, J.; Slusher, B. S. Kinetics and inhibition of glutamate carboxypeptidase II using a microplate assay. *Anal. Biochem.* **2002**, *310*, 50−54.

(14) Barinka, C.; Rinnova, M.; Sacha, P.; Rojas, C.; Majer, P.; Slusher, B. S.; Konvalinka, J. Substrate specificity, inhibition and enzymological analysis of recombinant human glutamate carboxypeptidase II. *J. Neurochem.* **2002**, *80*, 477−487.

(15) Cushman, D. W.; Cheung, H. S.; Sabo, E. F.; Ondetti, M. A. Design of potent competitive inhibitors of angiotensin-converting enzyme. Carboxyalkanoyl and mercaptoalkanoyl amino acids. *Biochemistry* **1977**, *16*, 5484−5491.

(16) Rong, S. B.; Zhang, J.; Neale, J. H.; Wroblewski, J. T.; Wang, S.; Kozikowski, A. P. Molecular modeling of the interactions of glutamate carboxypeptidase II with its potent NAAG-based inhibitors. *J. Med. Chem.* **2002**, *45*, 4140−4152.

(17) Vornov, J. J. Toxic NMDA-receptor activation occurs during recovery in a tissue culture model of ischemia. *J. Neurochem.* **1995**, *65*, 1681−1691.

(18) Bennett, G. J.; Xie, Y. K. A peripheral mononeuropathy in rat that produces disorders of pain sensation like those seen in man. *Pain* **1988**, *33*, 87−107.

JM049258G